A New Approach to Wideband Scene Projection

Russell M. Kurtz*, Alexander V. Parfenov, Ranjit D. Pradhan, Tin M. Aye, Gajendra D. Savant,

Nay Tun, Tin Win, and Jason Holmstedt

Physical Optics Corporation, Torrance, CA 90501

Axel Schindler

University of Stuttgart, Stuttgart, Germany

ABSTRACT

Advances in the development of imaging sensors depend upon (among other things) the testing capabilities of research laboratories. Sensors and sensor suites need to be rigorously tested under laboratory and field conditions before being put to use. Real-time dynamic simulation of real targets is a key component of such testing, as actual full-scale tests with real targets are extremely expensive and time consuming and are not suitable for early stages of development. Dynamic projectors simulate tactical images and scenes. Several technologies exist for projecting IR and visible scenes to simulate tactical battlefield patterns – large format resistor arrays, liquid crystal light valves, Eidophor type projecting systems, and micromirror arrays, for example. These technologies are slow, or are restricted either in the modulator array size or in spectral bandwidth. In addition, many operate only in specific bandwidth regions. Physical Optics Corporation is developing an alternative to current scene projectors. This projector is designed to operate over the visible, near-IR, MWIR, and LWIR spectra simultaneously, from 300 nm to 20 µm. The resolution is 2 megapixels, and the designed frame rate is 120 Hz (40 Hz in color). To ensure high-resolution visible imagery and pixel-to-pixel apparent temperature difference of 100°C, the contrast between adjacent pixels is >100:1 in the visible to near-IR, MWIR, and LWIR. This scene projector is designed to produce a flickerless analog signal, suitable for staring and scanning arrays, and to be capable of operation in a hardware-in-the-loop test system. Tests performed on an initial prototype demonstrated contrast of 250:1 in the visible with non-optimized hardware.

INTRODUCTION

In the decades since the introduction of the first electro-optical imaging sensors, quality and resolution of such sensors has increased greatly. In the past, these were typically forward-looking infrared (FLIR) sensors, sensing the heat signature of targets in either the mid-infrared (MWIR) band of 3-5 µm or the longwave infrared (LWIR) band of 8-12 µm. Such imaging systems were often tested by their capability to resolve simple targets (Figure 1). These led to systems designed for optimized modulation transfer function (MTF) and, for infrared systems, lowest minimum resolvable temperature difference (MRT). Unfortunately, good values of MTF and MRT did not necessarily result in good imaging systems. As imaging systems evolved into more complicated, higher resolution devices, better testing methods were required[1-3].

---

* rkurtz@poc.com, phone 1 310 320-3088, fax 1 310 320-4667, www.poc.com

Multisensor, Multisource Information Fusion: Architectures, Algorithms, and Applications 2005,
edited by Belur V. Dasarathy, Proceedings of SPIE Vol. 5813 (SPIE, Bellingham, WA, 2005)
0277-786X/05/$15 · doi: 10.1117/12.604142

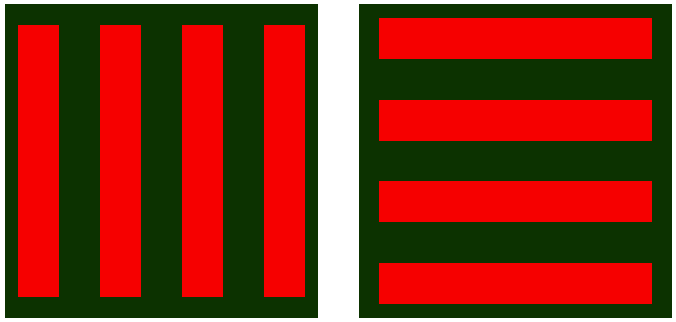

Figure 1
In past tests, imaging systems were often graded by their capability to measure MTF and MRT when viewing four-bar targets.

Television resolution increased, and imaging systems followed suit. The original Bradley thermal viewer, for example, had a resolution of 240×60 (horizontal × vertical) in 1985. The current Improved Bradley Acquisition Sensor (IBAS) has a projected resolution of 1920×960, a factor of 128 higher resolution than the original and nearly as high as the highest-resolution HDTV. As sensor quality improved, testing methods also improved[4]. Scene projectors, capable of showing realistic scenes to the sensor almost like a motion picture, are becoming the standard method of testing imaging systems.

The utility of scene projectors has led to many new technologies for testing sensors. Development of mobile scene projectors[5-7] led to their use in hardware-in-the-loop (HWIL) testing[8]. Improved technologies in emitter arrays and MEMS systems[9,10], together with improved image generation software[11], continue to lead the scene projector field toward systems whose resolution exceeds that of the highest-resolution imaging sensor they expect to test. In addition, many sensors are expanding their observational bandwidth, implementing sensor fusion to increase the total information available by fusing the output from sensors in several wavelength ranges[12]. The increase in sensor quality, addition of sensor fusion, and addition of HWIL to the test greatly increase the requirements on the scene projector used to test them, increasing resolution, brightness accuracy, and scene bandwidth requirements.

1. THEORY

1.1. Current Scene Generators

Among the most common scene projectors for use in the LWIR and MWIR are resistive emitter arrays[5,10,13], which only cover the area of the spectrum $\lambda > 2\ \mu m$. These systems cannot be used for near-ultraviolet (NUV), visible, or near-infrared (NIR) sensor testing. LED and laser diode arrays[13] are high-brightness, rapidly-adjustable sources that can span a large spectrum, but only at a few discrete wavelengths. Additionally, this technology is much more mature in the NIR and MWIR than in the NUV, visible, or LWIR regions of the spectrum. In the visible, the state of the art in scene projection uses spatial light modulators based on ferroelectric liquid crystal light valves[14]. While these systems are efficient and have excellent resolution, they do not work in the infrared or ultraviolet regions of the spectrum.

There are two high-efficiency methods of generating an ultrabroadband (NUV-visible-NIR-MWIR-LWIR) scene. One is to generate the scene independently in each wavelength region and combine the images. The other is to generate a single scene using purely reflective optics. Aligning multiple scenes is extremely difficult, and requires independent alignment and focus. A single reflective scene generator, with an external illumination source (which controls the spectral bands available) is a better solution. Multiple illumination sources—which can be aligned much more easily than multiple images, since the alignment requirements are much less stringent—can extend the scene generation bandwidth when necessary.

1.2. Reflective Scene Generation

To generate the simplest scene, a grayscale image, it is necessary to alter the brightness of each individual pixel. One way this is through MEMS-based digital micromirror devices (DMMDs). The Optical Sciences MAPS scene projector[15], similar to the Texas Instruments DLP™ array[16], has reflective coatings compatible with the visible and infrared bands. The MAPS has two main limitations. Its pixel size is ~15 µm, so there is some diffraction loss when the illumination wavelength is in the LWIR. The arrays have been shown to work in this wavelength band, but contrast is reduced – the DLP™ contrast is very high in the visible, and the MAPS would be expected to have an equally high contrast, but its contrast is reduced to ~90:1 in the MWIR and 40:1 in the LWIR[17]. The second limitation is its method of adjusting pixel intensity. Since the DLP™ is a digital device—it can only be fully on (flat) or fully off (tilted)—it varies apparent intensity by pulsewidth modulation (PWM). The amount of time per frame that the pixel is bright determines the apparent brightness of the frame. With the stated switching time of ~250 µs, at a frame rate of 30 Hz, the MAPS would have seven bits of intensity resolution. (DLP™-based systems have demonstrated switching times as low as 90 µs, which would give a full eight bits—256 gray levels—of dynamic range at a frame rate of 40 Hz.) The second disadvantage is only seen when a PWM-based system is used in testing a scanning sensor. In this case, instead of the smooth gradient that would be seen by a staring array the scanning system sees a series of black and white steps whose length corresponds to the width of the modulated pulse (Figure 2).

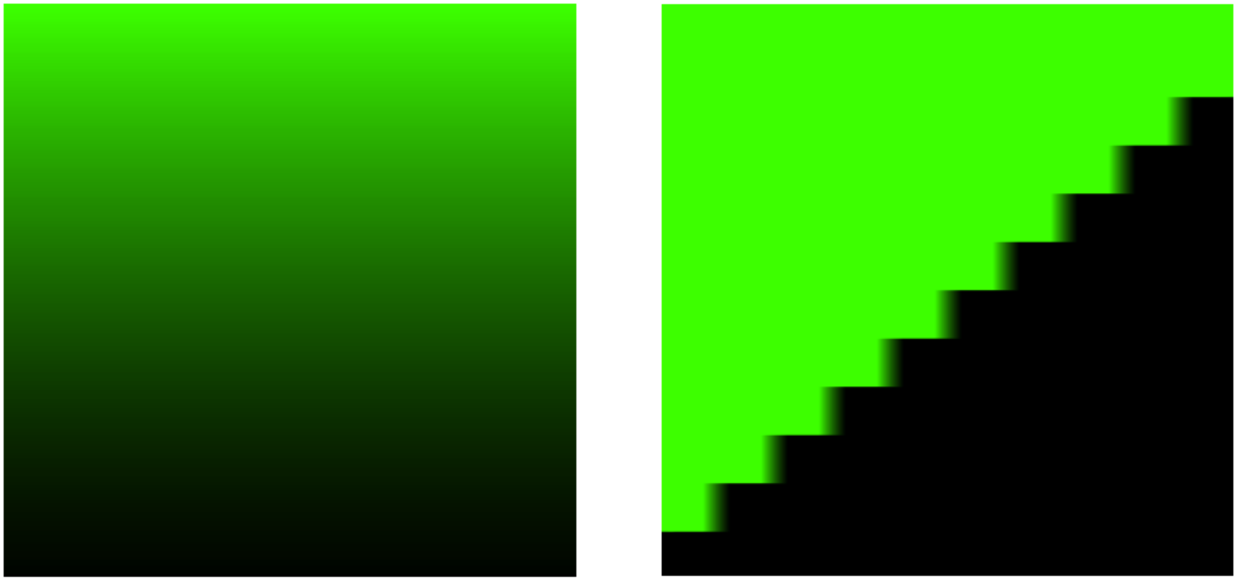

(a) (b)

Figure 2
If a PWM-based scene generator projects a gradient (a), it is seen as a gradient by staring sensors, but as a series of steps (b) by scanning sensors.

1.3. Reflective Scene Generation by Pixel Defocus

One major advantage of a DLP™-based scene generator is that it is a "staring" projector – its pixels are individually adjustable. This is also true of our new approach. Since we are avoiding digital methods of varying pixel intensity such as PWM, we needed to develop an analog pixel adjustment technique. We accomplish this through pixel defocus. Not only is each pixel directly accessible, necessary for HWIL testing, but each pixel maintains the same brightness throughout a frame, so this system can be used with scanning sensors. Pixel defocus depends on the spread of a reflected beam when it encounters a negative mirror (Figure 3). Incoming illumination is reflected at full intensity from a flat surface, but its intensity is reduced by defocus by a negative mirror.

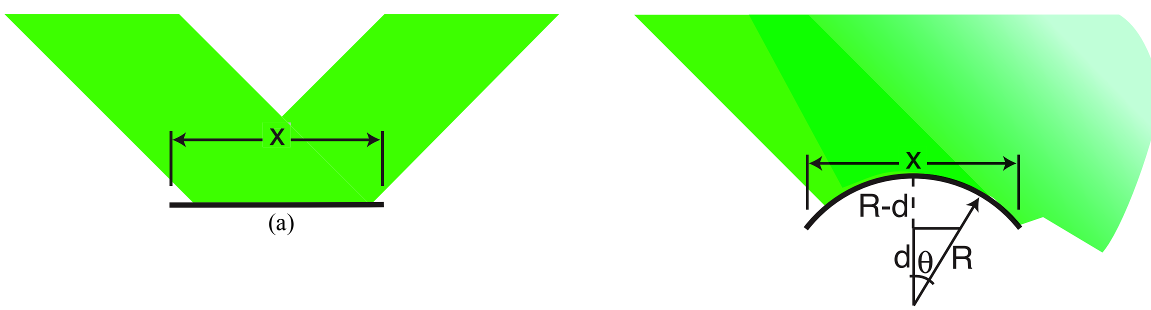

(a) (b)

Figure 3
Incoming illumination is reflected at full intensity by a flat pixel (a),
but the illumination intensity is reduced if the pixel is defocused (b).

As shown in Figure 3, deflection of a pixel into an arc whose radius is R results in maximum reflected ray deflection angle 2θ. The surface of the pixel is deflected an amount (R – d) over the flat area. The half-maximum deflection angle θ can be calculated from the arc length. From geometry we know the arc length is θ*R*. We can solve for θ by trigonometry:

$$\frac{x}{2R} = \sin\frac{\theta}{2} \ . \tag{1}$$

We can replace the sine by its approximation

$$\sin\theta \approx \theta - \frac{\theta^3}{6} \tag{2}$$

for angles expected in this scene generator. Combining eq. (1) with the arc length definition, we see

$$\theta R - (R - d) = \frac{\theta^3 R}{6} \ . \tag{3}$$

If we use a material whose length increases linearly with voltage,

$$x(V) = x_0 + \alpha V \ , \tag{4}$$

we note that the arc length θ*R* is equal to $x(V)$. Then the relationship between voltage and angle can be calculated from the arc length definition and eqs. (1) through (4):

$$\theta \approx \sqrt{\frac{6\alpha V}{x_0}} \ . \tag{5}$$

The pixel radius at a distance *z* from the scene generator surface is

$$r(z) = \frac{x_0}{2} + \theta z \approx \frac{x_0}{2} + \sqrt{6\alpha V \frac{z^2}{x_0}} \ , \tag{6}$$

and the ratio of the intensity produced by a defocused pixel to that produced by a flat pixel, at distance *z*, is

$$\frac{I(V)}{I(\text{flat})} \approx \frac{1}{1 + \sqrt{24\alpha V \frac{z^2}{x_0^3}}} \ . \tag{7}$$

The intensity of the pixel is inversely proportional to the square root of the applied voltage, and is approximately inversely proportional to the distance from the scene generator, and inversely proportional to the square root of the applied voltage. Eq. (7) is plotted in Figure 4 for pixel size $x_0 = 100$ µm, viewing distance $z = 50$ cm, and distance-voltage parameter $\alpha = 2\times10^{-8}\ V^{-1}$.

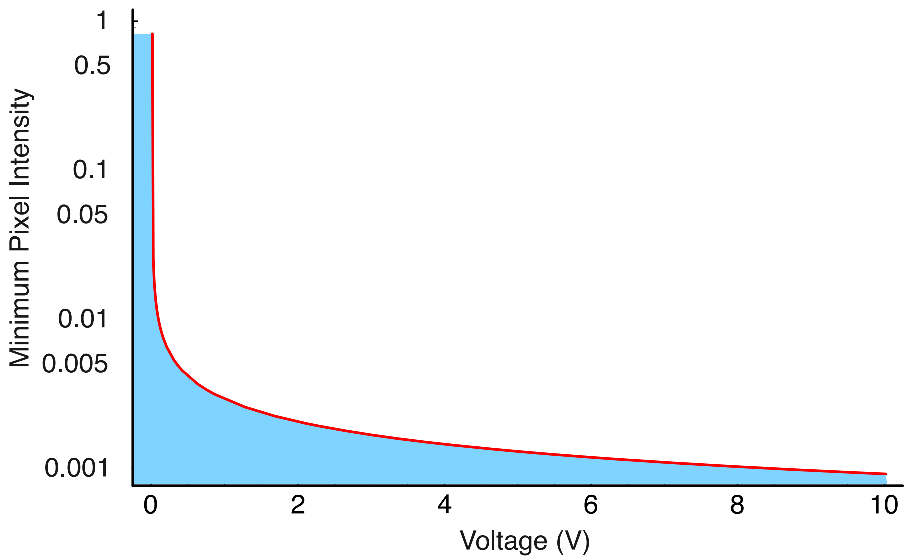

Figure 4
Pixel intensity is approximately inversely proportional to the square root of the applied voltage.

1.4. Correlation with Apparent Temperature

For the visible and NIR, the scene generator simply models the apparent brightness of images. In the MWIR and LWIR, however, the pixel brightness represents a temperature difference. The comparative brightness of two pixels is related to the apparent temperatures T_1 and T_2 of the pixels by

$$\frac{I(T_1)}{I(T_2)} = \frac{\exp\left(\dfrac{14388\ \mu\text{m K}}{\lambda T_1}\right) - 1}{\exp\left(\dfrac{14388\ \mu\text{m K}}{\lambda T_2}\right) - 1} \quad . \tag{8}$$

This is plotted for the MWIR and LWIR cases in Figure 5, with T_2 being room temperature (300 K).

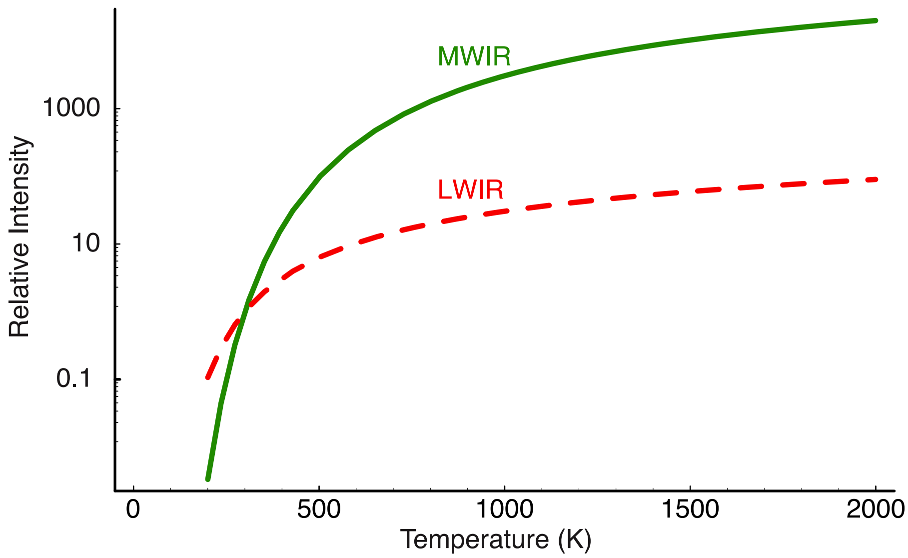

Figure 5
The pixel intensity, compared to that of a 300 K pixel, varies more slowly with temperature in the LWIR (dashed curve) than in the MWIR (solid curve).

2. EXPERIMENT

A simple, single-pixel scene generator (Figure 6) was designed to test the theory. The software and electronics were designed to be expandable to generate complete scenes. For prototyping convenience, the pixel was large (5 mm × 10 mm), so the drive voltage needed to be significantly higher than that calculated for Figure 4.

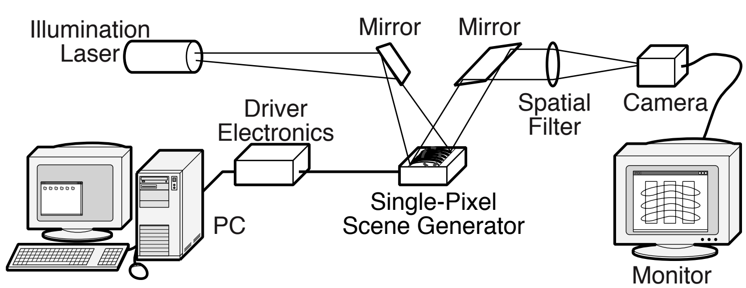

Figure 6
The scene generator principle was tested in a single-pixel system.

The prototype was tested under illumination by a 532-nm diode-pumped, frequency-doubled Nd:YVO_4 laser. Adjusting the pixel control voltage from 0 to 120 V resulted in an intensity variation of ~200, resulting in modulation contrast of >99%. Since the intensity variation is independent of wavelength, this system will produce equally large variations in the infrared. A factor of 200 variation in intensity corresponds to ~150°C temperature difference in the MWIR. Intensity calculations indicate that the maximum intensity variation will correspond to a pixel-to-background $\Delta T > 900$°C in the LWIR. It was possible to vary the intensity evenly over the entire brightness range, and the brightness did vary approximately as the inverse square root of the voltage (Figure 7).

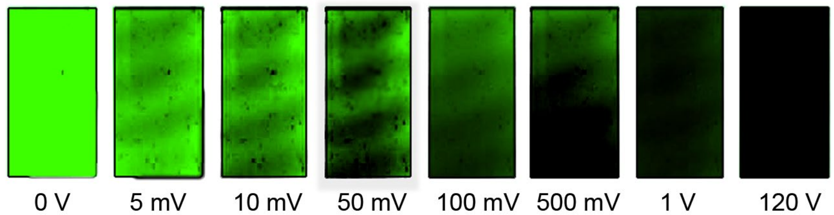

Figure 7
The intensity variation of the single pixel scene generator was approximately proportional to the inverse square root of applied voltage, shown here for voltage of (a) 0, (b) 5 mV, (c) 10 mV, (d) 50 mV, (e) 100 mV, (f) 500 mV, (g) 1 V, and (h) 120 V.

The actual and predicted intensities are shown in Table 1.

Table 1. Comparison of actual to predicted intensities from single pixel scene generator.

Voltage	0	5 mV	10 mV	50 mV	100 mV	500 mV	1 V	120 V
I_{pred}/I_0	100%	44%	35%	20%	15%	7%	5%	0.5%
I_{meas}/I_0	100%	55%	33%	19%	13%	8%	4%	0.4%

3. CONCLUSIONS

Physical Optics Corporation has developed a new approach to wideband scene projection. This reflective scene generator varies the intensity of each reflected pixel-by-pixel defocus, resulting in a high-quality, flicker-free image for projection into the sensor under test. Calculations indicate that this type of scene generator will have frame efficiency near 100%, ensuring its capability to work with all types of sensor (including both scanning and staring arrays). Moderate voltage levels (~10 V) can vary apparent pixel-to-pixel temperature by >200°C in the MWIR and >900°C in the LWIR, while maintaining an intensity contrast ratio of >200 across the full NUV-to-LWIR spectral band of 200 nm-14 µm. This scene generator can be designed to operate in any spectral band within this region, or any group of spectral bands simultaneously. The scene generation technique was demonstrated with a simple single-pixel experiment in which the measured pixel intensity closely matched the predicted intensity.

ACKNOWLEDGMENTS

This work was supported in part by the U.S. Army Test and Evaluation Command under Contract No. W31P4Q-04-C-R174.

REFERENCES

1. E.E. Burroughs Jr., W.R. Brown, H.M. Lastra, and F. Vuong, "Infrared Scene Projection, Synthetic Solution for Testing and Training FLIR Systems," *Interservice/Industry Training, Simulation & Education Conference*, 1999.
2. H.M. Lastra, E.E. Burroughs Jr., C. Vuong, and R. Brown, "IR Scene Projector Applications to Test and Training for FLIR Systems," *Army Test and Training Instrumentation Conference*, 1998.

3. E.E. Burroughs, R. Driggers, C. Halford, and M.A. Manzardo, "Beyond MRT," *SPIE International Symposium on Aerospace/Defense Sensing, Simulation, and Controls*, vol. 3063, 1997.
4. R. Driggers, M.A. Manzardo, E.E. Burroughs, C. Halford, and R. Vollmerhausen, "Managing Projector Aliasing for Tactical Infrared Imaging Systems," *SPIE Symposium on Aerospace/Defense Sensint, Simulation, and Controls*, vol. 3084, 1997.
5. D.B. Beasley, D.A. Saylor, and J.A. Buford Jr., "Overview of Dynamic Scene Projectors at the U.S. Army Aviation and Missile Command," *SPIE Technologies for Synthetic Environments: Hardware-in-the-Loop Testing*, vol. 4717, 136-147, 2002.
6. W.R. Brown, H.M. Lastra, F. Vuong, and G. Brooks, "Trade-Offs in Designing a Mobile Infrared Scene Projector," *SPIE International Symposium on Aerospace/Defense Sensing, Simulation, and Controls*, vol. 4027, Orlando, Florida, 2000.
7. E.E. Burroughs Jr., F. Vuong, W.R. Brown, and H.M. Lastra, "Tradeoffs in Designing a Mobile Infrared Scene Projector," *International Training and Evaluation Association Workshop*, 1999.
8. K.W. Zabel, R. Stone, L. Martin, R. Robinson, and M.A. Manzardo, "Utilization of a Mobile Infrared Scene Projector for Hardware-in-the-Loop Test and Evaluation of Installed Imaging Infrared Sensors," *SPIE International Symposium on Aerospace/Defense Sensing, Simulation, and Controls*, vol. 3697, Orlando, Florida, 1999.
9. B.E. Cole, B. Higashi, J.A. Ridley, J. Holmen, K. Newstrom, C. Zins, K. Nguyen, S.R. Weeres, B.R. Johnson, R.G. Stockbridge, R.L. Murrer Jr., E.M. Olson, T.P. Bergin, J.R. Kircher, and D.S. Flynn, "Innovations in IR Projector Arrays," *SPIE Technologies for Synthetic Environments: Hardware-in-the-Loop Testing V*, vol. 4027, 350-367, Orlando, Florida, 2000.
10. S.W. McHugh, R.M. Robinson, B. Parish, and J.T. Woolaway II, "MIRAGE: Large-Format Emitter Arrays 1024x1024 and 1024x2048," *SPIE Technologies for Synthetic Environments: Hardware-in-the-Loop Testing V*, vol. 4027, 399-408, Orlando, Florida, 2000.
11. K.H. Yu, A.A. Kostrzewski, T.M. Aye, S.A. Kupiec, T.P. Jannson, and G.D. Savant, "Scene Projector and Beowulf Parallel Microprocessor for Modeling and Simulation," *SPIE Cockpit Displays*, vol. 5080, 226-238, 2003.
12. A. Toet, "Detection of Dim Point Targets in Cluttered Maritime Backgrounds Through Multisensor Image Fusion," *SPIE Targets and Backgrounds VIII: Characterization and Representation*, vol. 4718, 118-129, Orlando, Florida, 2002.
13. D.B. Beasley and D.A. Saylor, "Application of Multiple IR Projector Technologies for AMCOM HWIL Simulations," *SPIE Technologies for Synthetic Environments: Hardware-in-the-Loop Testing IV*, vol. 3697, 223-231, Orlando, Florida, 1999.
14. Boulder Nonlinear Systems, "Analog Ferroelectric Liquid Crystals," 2001.
15. Optical Sciences Corporation, "Dynamic Infrared Scene Projectors," 2003, http://www.opticalsciences.com/Engineering/projectors/dmd/osc_dmdinfo.htm.
16. Texas Instruments, "DLP Technology," 2004, http://www.dlp.com.
17. D.B. Beasley, "Infrared Contrast of Optical Sciences Corp. MEMS-Based Scene Generator," personal communication to R.M. Kurtz, 2004.